Developmental Biology **208,** 30–43 (1999)
Article ID dbio.1998.9176, available online at http://www.idealibrary.com on IDEAL®

Essential Roles of Retinoic Acid Signaling in Interdigital Apoptosis and Control of BMP-7 Expression in Mouse Autopods

Valérie Dupé,*[,1] Norbert B. Ghyselinck,*[,1] Vilmos Thomazy,† László Nagy,† Peter J. A. Davies,† Pierre Chambon,* and Manuel Mark*[,2]

**Institut de Génétique et de Biologie Moléculaire et Cellulaire (IGBMC), CNRS/INSERM/ULP/ Collège de France, B.P. 163, 67404 Illkirch Cedex, C.U de Strasbourg, France; and †Department of Integrative Biology and Pharmacology, University of Texas at Houston, School of Medicine, Houston, Texas 77030*

We previously reported that mice lacking the RARγ gene and one or both alleles of the RARβ gene (i.e., RAR$\beta^{+/-}$/RAR$\gamma^{-/-}$ and RAR$\beta^{-/-}$/RAR$\gamma^{-/-}$ mutants) display a severe and fully penetrant interdigital webbing (soft tissue syndactyly), caused by the persistence of the fetal interdigital mesenchyme (Ghyselinck *et al.*, 1997, *Int. J. Dev. Biol.* 41, 425–447). In the present study, these compound mutants were used to investigate the cellular and molecular mechanisms involved in retinoic acid (RA)-dependent formation of the interdigital necrotic zones (INZs). The mutant INZs show a marked decrease in the number of apoptotic cells accompanied by an increase of cell proliferation. This marked decrease was not paralleled by a reduction of the number of macrophages, indicating that the chemotactic cues which normally attract these cells into the INZs were not affected. The expression of a number of genes known to be involved in the establishment of the INZs, the patterning of the autopod, and/or the initiation of apoptosis was also unaffected. These genes included *BMP*-2, *BMP*-4, *Msx*-1, *Msx*-2, 5′ members of Hox complexes, *Bcl2*, *Bax*, and *p53*. In contrast, the mutant INZs displayed a specific, graded, down-regulation of tissue transglutaminase (tTG) promoter activity and of stromelysin-3 expression upon the removal of one or both alleles of the RARβ gene from the RARγ null genetic background. As retinoic acid response elements are present in the promoter regions of both tTG and stromelysin-3 genes, we propose that RA might increase the amount of cell death in the INZs through a direct modulation of tTG expression and that it also contributes to the process of tissue remodeling, which accompanies cell death, through an up-regulation of stromelysin-3 expression in the INZs. Approximately 10% of the RAR$\beta^{-/-}$/RAR$\gamma^{-/-}$ mutants displayed a supernumerary preaxial digit on hindfeet, which is also a feature of the *BMP-7* null phenotype (Dudley *et al.*, 1995, *Genes Dev.* 9, 2795–2807; Luo *et al.*, 1995, *Genes Dev.* 9, 2808–2820). *BMP-7* was globally down-regulated at an early stage in the autopods of these RAR double null mutants, prior to the appearance of the digital rays. Therefore, RA may exert some of its effects on anteroposterior autopod patterning through controlling *BMP-7* expression.

Key Words: **limb development; retinoic acid receptors; tissue transglutaminase; stromelysin-3, BMP-7.**

INTRODUCTION

The effects of retinoids, the biologically active derivatives of vitamin A, are transduced by nuclear receptors, the RARs[3] (α, β, and γ) and the RXRs (α, β, and γ). RXR:RXR homodimers and RXR:RAR heterodimers bind cognate regulatory DNA sequences, or response elements, and act as ligand-inducible transcriptional regulators (Chambon,

[1] Should be considered equal first authors.

[2] To whom correspondence should be addressed. Fax: 33+ 3 88 65 32 03.

[3] Abbreviations used: ANZ, anterior necrotic zone; BMP, bone morphogenetic protein; CRABP, cellular retinoic acid binding protein; INZ, interdigital necrotic zone; PNZ, posterior necrotic zone; PCD, physiological cell death; RA, retinoic acid; RAR, retinoic acid receptor; RXR, retinoid X receptor; tTG, tissue transglutaminase; WT, wild-type.

0012-1606/99 $30.00

1996). Simultaneous knock-out of two RAR isotypes, or of RXRα and a given RAR isotype (α, β, or γ), leads to numerous developmental defects which, altogether, recapitulate the fetal vitamin A deficiency syndrome, thus demonstrating that these receptors indeed transduce the retinoid signal during embryonic development (Lohnes *et al.*, 1994; Mendelsohn *et al.*, 1994; Kastner *et al.*, 1994, 1997; Ghyselinck *et al.*, 1997). Interestingly, the phenotypic analysis of retinoid receptor single and compound null mutants has revealed many additional abnormalities which were not known to be associated with an impaired vitamin A function, for instance, interdigital webbing (soft tissue syndactyly) caused by the persistence of the fetal interdigital mesenchyme (Ghyselinck *et al.*, 1997).

All three RARs (α, β, and γ) are expressed in mouse autopods during the period of regression of the interdigital mesenchyme. The expression of RARα transcripts and proteins is ubiquitous; RARγ transcripts and proteins are detected mainly in the precartilaginous anlagen of the digits and in the autopod's ectoderm (Dollé *et al.*, 1989b; Ghyselinck *et al.*, 1997). RARβ transcripts, proteins, and RARβ2 promoter activity are confined to the interdigital, anterior, and posterior necrotic zones (INZ, ANZ, and PNZ) (Dollé *et al.*, 1989b; Ghyselinck *et al.*, 1997; Mendelsohn *et al.*, 1991). RXRα, the main heterodimerization partner of the three RARs during embryonic development (Kastner *et al.*, 1997), is also expressed ubiquitously in the autopod (Dollé *et al.*, 1994).

Interdigital webbing is observed in a small fraction of RXR$\alpha^{+/-}$, RAR$\alpha^{-/-}$, and RAR$\gamma^{-/-}$ mutants (Kastner *et al.*, 1997; Lohnes *et al.*, 1994; Lufkin *et al.*, 1993). Its penetrance and severity increase markedly in RXR$\alpha^{+/-}$/RAR$\alpha^{+/-}$ and RXR$\alpha^{+/-}$/RAR$\gamma^{+/-}$ compound heterozygote mice, indicating that RXRα:RARα and RXRα:RARγ heterodimers are involved in the separation of the digits (Kastner *et al.*, 1997). In contrast, RAR$\beta^{-/-}$ mice have normal limbs (Ghyselinck *et al.*, 1997) and the penetrance of interdigital webbing is identical in RXR$\alpha^{+/-}$ and RXR$\alpha^{+/-}$/RAR$\beta^{-/-}$ mutants (Kastner *et al.*, 1997). Since the limbs of RAR$\alpha^{-/-}$/RAR$\beta^{-/-}$ mutants are also normal (Ghyselinck *et al.*, 1997), the lack of effects of the RARβ knock-out on limb morphogenesis is not simply the consequence of a functional redundancy with RARα in the interdigital mesenchyme. Instead, the absence of digit separation observed in all RAR$\beta^{+/-}$/RAR$\gamma^{-/-}$ and RAR$\beta^{-/-}$/RAR$\gamma^{-/-}$ mutants strongly suggests the necessity, for proper digit separation, of short-range interactions between tissues expressing RARγ (i.e., precartilaginous condensation of the digits and autopod's ectoderm) and RARβ (interdigital mesenchyme) (Ghyselinck *et al.*, 1997).

Compound RARβ/RARγ mutants have been used here to investigate the cellular and molecular mechanisms involved in retinoic acid (RA)-dependent digit separation. We have compared, in wild-type and RARβ-RARγ compound mutant autopods, the distribution of dying and proliferating cells and the expression patterns of several genes implicated (i) in the establishment of the interdigital necrotic zones (*BMP-2*, *4*, and *7*, and *Msx1* and *2* genes) and/or in the patterning of the autopod (5′ members of Hox complexes), (ii) in the effector phase of apoptosis (*Bcl2*, *Bax*, *p53*, and tissue transglutaminase genes), and (iii) in tissue remodeling processes (stromelysin-3 gene).

MATERIALS AND METHODS

Mice

RAR$\beta^{+/-}$/RAR$\gamma^{+/-}$ mice (Ghyselinck *et al.*, 1997) were intercrossed to generate RAR$\beta^{+/-}$/RAR$\gamma^{-/-}$ and RAR$\beta^{-/-}$/RAR$\gamma^{-/-}$ mutant fetuses which were recovered at the frequency of 1/8 or 1/16, respectively. Mice were mated overnight and the next morning was considered 0.5 days postcoitum (embryonic day 0.5, E0.5). Pregnant females were sacrificed by cervical dislocation. Embryos were collected by cesarian section and yolk sacs were taken for DNA extraction. Genotypes were determined by Southern blotting as previously described (Ghyselinck *et al.*, 1997; Lohnes *et al.*, 1993).

Detection of Cell Death

The extent of cell death was assessed on whole limbs by staining, immediately after dissection, with a 1/50,000 solution of Nile blue sulfate in PBS for 30 min at 24°C. Following staining, embryos were rinsed for 30 min in PBS and then immediately photographed. For detection of apoptotic cells, embryos were first fixed in 4% paraformaldehyde in PBS for 12 h at 4°C and then embedded in paraplast. Histological sections were mounted on 0.1% polylysine (Sigma, St. Louis, MO; MW 350,000) coated slides. Apoptotic cells were identified using an "Apoptag" *in situ* apoptosis detection kit (Oncor, Gaithersburg, MD) according to the manufacturer's instructions. Peroxydase was detected using diaminobenzydine and the sections were counterstained with methyl green.

Immunohistochemical Detection of Macrophages and of Bcl2

Embryos were fixed for 12 h at 24°C in Bouin's fluid and then thoroughly rinsed in 70% ethanol prior to further dehydratation and wax embedding. Histological sections, 7 μm thick, were mounted on 0.1% polylysine coated slides. To detect macrophages, the sections were first treated for 1 h at 24°C in PBS–0.05% Tween 20 containing 5% goat serum to block nonspecific antibody binding and then incubated with the macrophage-specific rat anti-mouse monoclonal F4/80 antibody (Austyn and Gordon, 1981) at a dilution of 1/20 in PBS for 90 min at 24°C. For detection of Bcl2, the sections were first incubated in target retrieval solution (Dako, Carpinteria, CA) for 30 min at 95°C, washed twice in PBS, and then preblocked for 30 min in a TNK buffer (0.1 Tris, pH 7.6; 0.55 NaCl; 10 mM KCl) containing 2% bovine serum albumin, 0.1% Triton X-100, and 1% normal goat serum (Krajewski *et al.*, 1994). An antiserum against human Bcl2 (Pharmingen, San Diego, CA) was added to the slides at a dilution of 1/800 in the supplemented TNK buffer and incubated for 16 h at 4°C. After being rinsed in PBS (3 × 5 min), F4/80 and anti-Bcl2 binding sites were revealed using an ABC system (Vector, Burlingame, CA) according to the manufacturer's instructions. The sections were slightly counterstained with Harris's hematoxylin.

Labeling of S-Phase Nuclei

Bromodeoxyuridine (BrdU, Sigma), dissolved in PBS, was injected intraperitoneally at a dose of 50 mg per kilogram of body weight. The mice were killed 2 h later, and the limbs were fixed in Bouin's fluid for 24 h at 24°C and then embedded in paraffin. BrdU incorporation was detected by using an anti-BrdU monoclonal antibody (Boehringer Mannheim, Germany) and immunoperoxidase labeling.

Whole-Mount in Situ Hybridizations

Whole-mount *in situ* RNA hybridization procedures were carried out as described by Conlon and Rossant (1992). Mutant limbs and contralateral wild-type limbs were processed in the same tube and were hybridized for the same length of time and under the same conditions. The probes used in this study have been described elsewhere: *BMP-2* (Lyons *et al.*, 1990), *BMP-4* (Jones *et al.*, 1991), *BMP-7* (Arkell *et al.*, 1997), *Msx-1* (Hill *et al.*, 1989), *Msx-2* (Coelho *et al.*, 1991), *Hoxd-11*, *Hoxd-12* (Dollé *et al.*, 1989a), *Hoxa-13* (Warot *et al.*, 1997), *Hoxd-13* (Dollé *et al.*, 1991), *p-53* (Jenkins *et al.*, 1984), *Bax* (Oltvai *et al.*, 1993), and stromelysine-3 (Lefebvre *et al.*, 1992) probes. Limbs were photographed in 50% glycerol in PBS and, in general, mutants and wild-type were taken on the same picture.

Tissue Transglutaminase Transgenic Mice and Detection of β-Galactosidase Activity

Homozygous transgenic males (tg/tg), containing 3.8 kb of tTG promoter driving the expression of the β-galactosidase reporter gene (LacZ) (Nagy *et al.*, 1997), were crossed with RAR$\beta^{+/-}$/RAR$\gamma^{+/-}$ double heterozygous mutant females. RAR$\beta^{+/-}$/RAR$\gamma^{+/-}$/tg/0 males were subsequently crossed with RAR$\beta^{+/-}$/RAR$\gamma^{+/-}$ females, giving 1 of 32 fetuses doubly homozygous for the RARβ and RARγ null mutations and carying one copy of the transgene. Embryos were fixed in 2% formaldehyde for 1 h at 4°C and then washed with PBS (2 × 15 min) and stained for 16 h at 30°C in a solution containing 1 mg/ml of X-gal, 5 mM $K_3Fe(CN)_6$, 5 mM $K_4Fe(CN)_6$, 2 mM $MgCl_2$ in PBS, postfixed in 4% paraformaldehyde or in Bouin's fluid, and stored in 70% ethanol. The limbs were then eventually paraffin-embedded, serially sectioned, and counterstained for 1 min with a 0.01% solution of Safranin O (CI: 50240) in distilled water.

RESULTS

For the sake of simplicity, homozygous RARβ and RARγ null mutants are designated hereafter as Aβ and Aγ, the "$^{-/-}$" sign indicating homozygocity being omitted. Thus, for instance, RAR$\beta^{-/-}$/RAR$\gamma^{-/-}$ and RAR$\beta^{+/-}$/RAR$\gamma^{-/-}$ mutants are referred to as Aβ/Aγ and A$\beta^{+/-}$/Aγ mutants, respectively. At least two anterior and two posterior limbs from different fetuses were examined for each genotype and developmental stage.

Reduction of Cell Death and Increased Cell Proliferation in the Interdigital Mesenchymal Cells of RARβ/RARγ Mutants

In the wild-type (WT) autopod, physiological cell death (PCD) starts at E12.5 in the interdigital mesenchyme underlying the ectoderm and spreads proximally in the INZs, peaking at E14.0 in the forelimb and at E14.5 in the hindlimb. Digit separation is completed by E15.0 and E15.5 in the anterior and posterior limbs, respectively (Zakeri and Ahujo, 1994; Waneck *et al.*, 1989; Maconnachie, 1979). The limbs of Aβ/Aγ mutants were analyzed at E12.5 and E13.5, i.e., at developmental stages at which they are morphologically undistinguishable from their WT counterparts.

Nile blue sulfate, a vital dye accumulating in dying cells, was used to assess the three-dimensional extent of cell death in E13.5 autopods (Zakeri and Ahuja, 1994). In Aβ/Aγ mutants, the amount of blue stained cells was markedly reduced in the INZs between all digits in both fore- and hindlimbs (Figs. 1a and 1b and data not shown); in contrast, the dye accumulated normally in the anterior and posterior necrotic zones (compare ANZ and PNZ in Figs. 1a and 1b). This observation indicates that the interdigital webbing observed in E15.5 to E18.5 Aβ/Aγ mutants (Ghyselinck *et al.*, 1997) is caused, at least in part, by a decrease in cell death in the mesenchyme of the INZs. Apoptosis, which is responsible for cell death in the INZs (Schweichel and Merker, 1973; Hinchliffe, 1981), is, in general, accompanied by the endonucleolytic cleavage of chromosomal DNA into nucleosome-size units which can be detected using a DNA labeling assay (TUNEL, terminal desoxynucleotidyl transferase-mediated dUTP nick end labeling) (Gavrieli *et al.*, 1992). The number of TUNEL-positive nuclei or nuclear fragments was markedly and selectively reduced in E13.5 Aβ/Aγ INZs (compare Fig. 1c to 1d), but not in the anterior necrotic zone (ANZ) and posterior necrotic zone (PNZ) and in the forming joints of the phalanges (J) (Figs. 1c and 1d and data not shown). The percentage of cells containing DNA nicks was established by nuclear counts in the second interdigital space of three E13.5 WT and three Aβ/Aγ forelimbs from different fetuses. Every third section was analyzed, and about 2000 nuclei were scored in each limb. In the INZ of Aβ/Aγ mutants 3.7± 1.3% of the mesenchymal cells were undergoing apoptosis versus 19.1±1.2% in the WT INZ. In A$\beta^{+/-}$/Aγ mutants which also display a completely penetrant interdigital webbing (Ghyselinck *et al.*, 1997), the decrease of cell death in the INZs (Nile blue staining and TUNEL assay) was less pronounced than in the double null mutants (data not shown).

Apoptotic cells in the INZs are rapidly phagocytosed by monocyte-derived macrophages which react specifically with the monoclonal antibody F4/80 (Hopkinson-Woolley *et al.*, 1994). In E13.5 WT autopods, macrophages were colocalized with apoptotic cells and many of them were full of phagocytosed cellular debris (arrows in Fig. 1e; see also Hopkinson-Woolley *et al.*, 1994). In E13.5 Aβ/Aγ autopods, F4/80-positive cells were as numerous as in their WT counterparts. However, they appeared more dispersed and most of them did not contain cell debris (arrowheads, compare Fig. 1e to 1f). Therefore, the lack of PCD in Aβ/Aγ mutants is not secondary to a failure of migration of macrophages to the INZs.

Bromodeoxyuridine incorporation into S phase nuclei

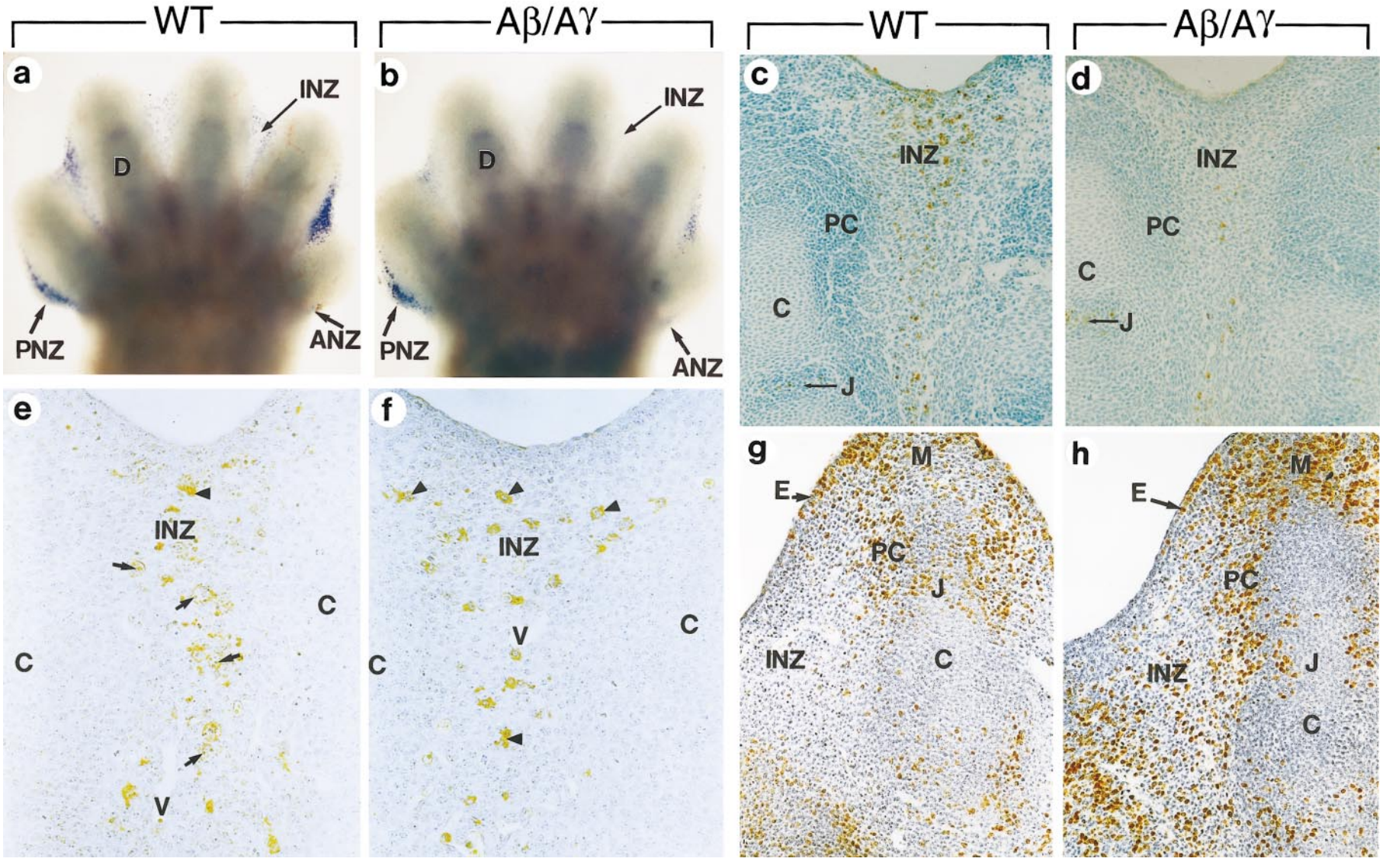

FIG. 1. Comparison of cell death (a–d), macrophage distribution (e and f), and cell proliferation (g and h) in E13.5 wildtype (WT) and Aβ/Aγ forelimbs. (a and b) Dorsal views of whole-mounts; (c–h) histological sections. (a and b) Nile blue sulfate staining of dying cells. (c and d) *In situ* detection of fragmented DNA; methyl green counterstain. (e and f) Immunostaining with the macrophage-specific antibody F4/80; hematoxylin counterstain. (g and h) *In situ* detection of S phase nuclei; hematoxylin counterstain. ANZ, anterior necrotic zone; C, cartilage condensation; D, digit; E, ectoderm; J, forming joint; INZ, interdigital necrotic zone; M, mesenchyme at the tips of the growing digits; PC, perichondrium; PNZ, posterior necrotic zone; V, capillary. Magnifications, ×60 (a and b); ×160 (c and d); ×340 (e and f); ×200 (g–h).

was used to assess cell proliferation. At E12.5, the patterns of cell proliferation in WT and Aβ/Aγ autopods were indistinguishable (data not shown). In E13.5 WT and Aβ/Aγ autopods (Figs. 1g and 1h) numerous BrdU-labeled nuclei were observed in the perichondrium (PC), in the mesenchyme at the tips of the growing digits (M) and its overlying ectoderm (E), as well as in the forming joints (J); positive nuclei were scarce in the cartilaginous condensations of the digits (C). Labeling indices were determined by nuclear counts in the fourth interdigital space of three E13.5 WT and three Aβ/Aγ forelimbs from different fetuses. Every third section was analyzed and about 1300 nuclei were scored in each limb. In the WT interdigital mesenchyme only 5.4 ± 0.65 of the cells were in S phase versus 23.5 ± 1.7% in the Aβ/Aγ mutant mesenchyme. Thus, the down-regulation of cell proliferation which occurs at E13.5 in the WT INZs was not observed in their Aβ/Aγ counterparts (compare INZ in Figs. 1g and 1h).

Distribution of BMP, Msx, and Hox Gene Transcripts in RARβ/RARγ Mutant Autopods

Putative extracellular signals for triggering interdigital apoptosis include *BMP-2, BMP-4,* and *BMP-7,* all of which are expressed in the interdigital mesenchyme before and during its regression in mouse and chick autopods (reviewed in Hogan, 1996; Lyons *et al.,* 1990; Francis *et al.,* 1994; Helder *et al.,* 1995). Beads soaked in BMP-2, BMP-4, or BMP-7 accelerate PCD when implanted in the interdigital region and, when implanted at the tip of a growing digit, lead to the formation of an ectopic area of apoptosis (Ganan *et al.,* 1996, Macias *et al.,* 1997). Moreover, blocking BMP signaling, by expressing a dominant-negative BMP receptor in the chicken, results in greatly reduced interdigital apoptosis and subsequently in webbed feet (Zou and Niswander, 1996; Yokouchi *et al.,* 1996). It is noteworthy that BMP-7 null mutant mice do not display webbed digits (Luo *et al.,* 1995); this may reflect a functional redundancy with other members of the family (e.g., BMP-2 and/or BMP-4). The distribution patterns of *BMP-2, BMP-4,* and *BMP-7* transcripts were analyzed in E12.5 and E13.5 by whole-mount *in situ* hybridization. *BMP-2* and *BMP-4* were similarly expressed in WT and Aβ/Aγ autopods. In accordance with previous data (Hogan, 1996), *BMP-2* transcripts were detected in the INZs, ANZ, and PNZ (e.g., Fig. 2a), whereas *BMP-4* was strongly expressed in the ANZ, PNZ, and mesenchymal cells at the tip of the growing digits (arrowhead in Fig. 2b) and, more weakly, in the INZs. In contrast, *BMP-7,* which is normally expressed in all three types of necrotic zones (Figs. 2c and 2d; Luo *et al.,* 1995; Hogan, 1996) was consistently decreased in Aβ/Aγ autopods at E12.5 (Fig. 2c) and E13.5 (Fig. 2d). This decrease was not observed in $A\beta^{+/-}$/Aγ autopods (data not shown).

We next analyzed the expression of homeobox genes which are thought to be implicated in interdigital cell death. *Msx*-1 and *Msx*-2 are expressed in the interdigital and marginal regions of the autopods before and during the establishment of the INZs, ANZ, and PNZ (Hill *et al.,* 1989; Coelho *et al.,* 1991, 1992; Robert *et al.,* 1991; Suzuki *et al.,* 1991). The inhibition of cell death induced by TGFβ in interdigital regions is preceded by down-regulation of *BMP-4, Msx-1, and Msx*-2 (Ganan *et al.,* 1996). Furthermore, BMP-4-induced *Msx*-2 expression has been associated with PCD in mouse rhombencephalic neural crest cells (Graham *et al.,* 1994). However, the pattern of expression of *Msx*-1 and *Msx*-2 was not altered in E12.5 and E13.5 Aβ/Aγ autopods (not shown).

Interdigital webbing is found in the forelimbs of *Hoxa-*$13^{+/-}$ mutants and in both fore- and hindlimbs of *Hoxa-*$13^{+/-}$/*Hoxd-*$13^{+/-}$ compound mutants (Fromental-Ramain *et al.,* 1996). Synpolydactyly is observed in mice lacking both *Hoxa-13* and *Hoxd-13* (Fromental-Ramain *et al.,* 1996) or carrying a targeted deletion of *Hoxd-13, Hoxd-12,* and *Hoxd-11* (Dollé *et al.,* 1993; Davis and Capecchi, 1994; Favier *et al.,* 1996; Zakany and Duboule, 1996). Interestingly, systemic administration of RA induces rapid changes in the *Hoxd-11* and *Hoxd-13* expression patterns, even at late stages of autopodal development (Wood *et al.,* 1996). At E12.5 and E13.5, *Hoxa-13* and *Hoxd-13* expression extends to the anterior margin of the autopod (Fig. 2 and data not shown), while *Hoxd-12* and *Hoxd-11* expression displays an anterior boundary between the first and the second digits (arrowhead in Fig. 2e; and data not shown). At E13.5, *Hoxa-13, Hoxd-13, Hoxd-12,* and *Hoxd-11* transcripts are not detected in cartilage condensations, but persist in the perichondrium, the forming joints, and the interdigital spaces, as previously described in the chick limb bud (Ros *et al.,* 1994). At E12.5 and E13.5 expression of these *Hox* genes was normal in autopods of Aβ/Aγ mutants (Fig. 2 and data not shown).

Expression of Intracellular Regulators of Cell Death in RARβ/RARγ Mutant Autopods

Overexpressed *Bcl2* increases the survival of numerous cells types exposed to a variety of apoptotic stimuli both *in vitro* and *in vivo* (Nunez *et al.,* 1990; Vaux *et al.,* 1988). Decreased *Bcl2* expression is observed in systems that are stimulated to undergo apoptosis (Merino *et al.,* 1994; Veis *et al.,* 1993), in particular in retinoid-induced cell death of human myeloid leukemic cell lines (Nagy *et al.,* 1996b; Agarwal and Mehta, 1997; Monczak *et al.,* 1997). The interaction of Bcl2 with Bax is thought to represent a key mechanism of the intracellular control of apoptosis, as it is widely held that Bcl2/Bax heterodimers promote survival, whereas Bax homodimers can directly trigger apoptosis (Oltvai *et al.,* 1993). In the autopod of WT fetuses at E12.5 and E13.5, the Bcl2 protein was detected exclusively in the cartilaginous condensations (C, Fig. 3a) in accordance with a previous immunohistochemical study using a different antibody (Novack and Korsmeyer, 1994). *Bax* transcripts were confined to the ANZ, PNZ, and INZs (Fig. 3b). Expression of the Bcl2 protein and of *Bax* transcripts was apparently identical in the mutant and WT autopods (data not shown).

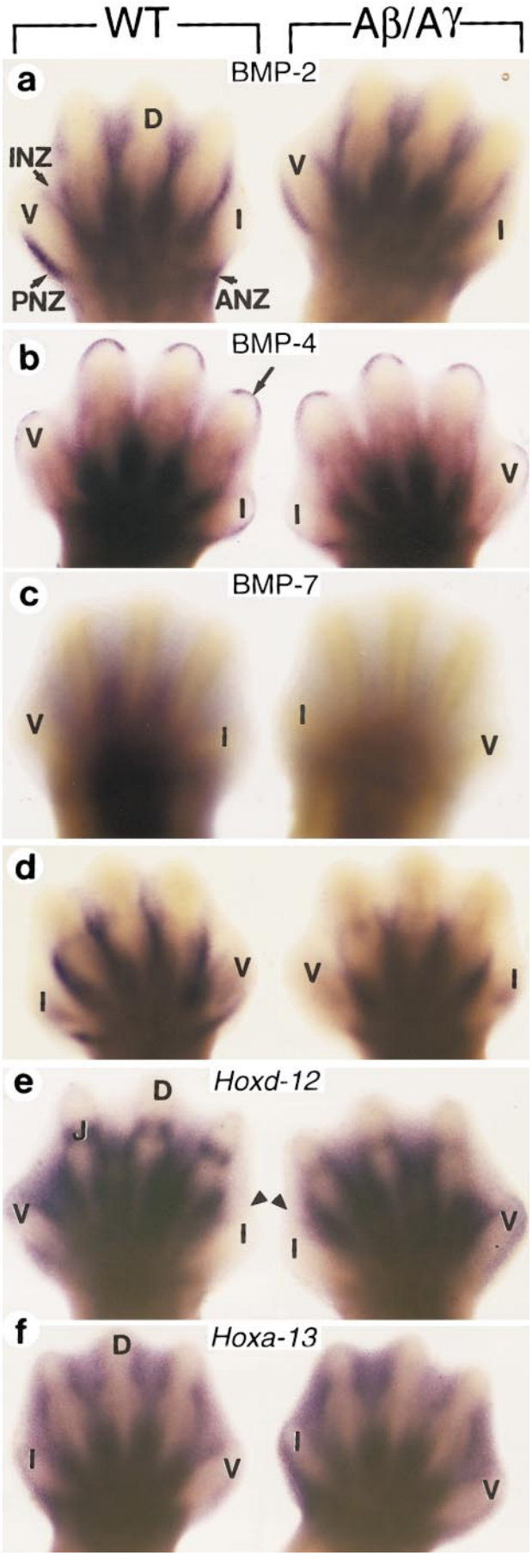

P53 can promote apoptosis in several cell types (Debbas and White, 1993; Morgenbesser *et al.*, 1994). P53 is a direct transcriptional regulator of the human *Bax* gene (Miyashita and Reed, 1995), and mice deficient in p53 exhibit an increase in Bcl2 and a decrease in Bax protein levels in several tissues (Miyashita *et al.*, 1994). At E12.5 and E13.5, similar levels of *p53* transcripts were present in all necrotic zones (ANZ, PNZ, and INZ in Fig. 3c), in the perichondrium (P), and in the forming joints (J) in both WT and Aβ/Aγ autopods (Fig. 3c and data not shown).

Tissue Transglutaminase and Stromelysin-3 Are Down-Regulated in RARβ/RARγ Mutants

Tissue transglutaminase (tTG) accumulates to high levels in cells committed to apoptosis (Fesus *et al.*, 1991; Piacentini *et al.*, 1991). In E14.0 transgenic mouse limbs expressing the LacZ gene under the control of the tTG promoter, β-galactosidase activity was detected in the ectoderm at the tip of the growing digits (E), in the ANZ, PNZ, and INZs between digits 2 and 5 in both fore- and hindlimbs (Fig. 4e and data not shown, see also Nagy *et al.*, 1997). It is noteworthy that in these three types of necrotic zones the pattern of transgene expression faithfully recapitulated the distribution of the endogenous enzyme (Nagy *et al.*, 1997). Expression of the transgene in the INZs was not confined to cells exhibiting the morphologic hallmarks of apoptosis (Nagy *et al.*, 1997). Instead, the majority of the tTG transgene-expressing cells in the INZs showed normal nuclear profiles on histological sections (Fig. 5a); such cells are likely to be biased toward apoptosis (Nagy *et al.*, 1997). X-gal staining was specifically decreased in the INZs of E14.0 $A\beta^{+/-}/A\gamma$ autopods (Fig. 4f), while it was almost abrogated in the INZs of Aβ/Aγ autopods (Figs. 4g and 5b). Serial histological sections revealed a consistent and strong decrease of β-galactosidase activity within individual interdigital mesenchymal cells of Aβ/Aγ mutants (compare Figs. 5a and 5b). Therefore, the decrease in X-gal staining observed on whole mounts of $A\beta^{+/-}/A\gamma$ and Aβ/Aγ autopods (Figs. 4e–4g) does not reflect a decrease in the number of cells expressing the transgene, but rather a reduced expression of tTG in each cell. Interestingly, there was no decrease in tTG promoter activity in other places where the tTG transgene is expressed at E14.0 and E12.5 including the calvaria (Ca), snout (S) (Figs. 4a and 4b), and ANZ and PNZ (compare Figs. 4c and 4e to 4d and 4g). Therefore, there is a correlation between the decrease of the tTG promoter activity at the cellular level and the commitment to cell death in the interdigital regions of Aβ/Aγ mutants.

FIG. 2. Distribution of *BMP-2*, *4*, and *7* and of *Hoxd-12* and *Hoxa-13* transcripts in WT and Aβ/Aγ forelimbs at E12.5 (c) and/or E13.5 (a, b, and d–f). (c and d) Note the global down-regulation of *BMP-7* at these two developmental stages. (e and f) Note that the expression domain of *Hoxa-13* encompasses the mesenchyme of the whole autopod with exception of the cartilaginous blastema, whereas that of *Hoxd-12* displays an anterior limit in the first interdigital space (arrowhead) in both WT and Aβ/Aγ autopods. ANZ, anterior necrotic zone; D, digit; INZ, interdigital necrotic zone; PNZ, posterior necrotic zone; I and V, digits 1 and 5. The arrow in (b) points to the mesenchyme at the tips of the growing digits. Magnifications, ×45 (a, b, and d–f); ×200 (c).

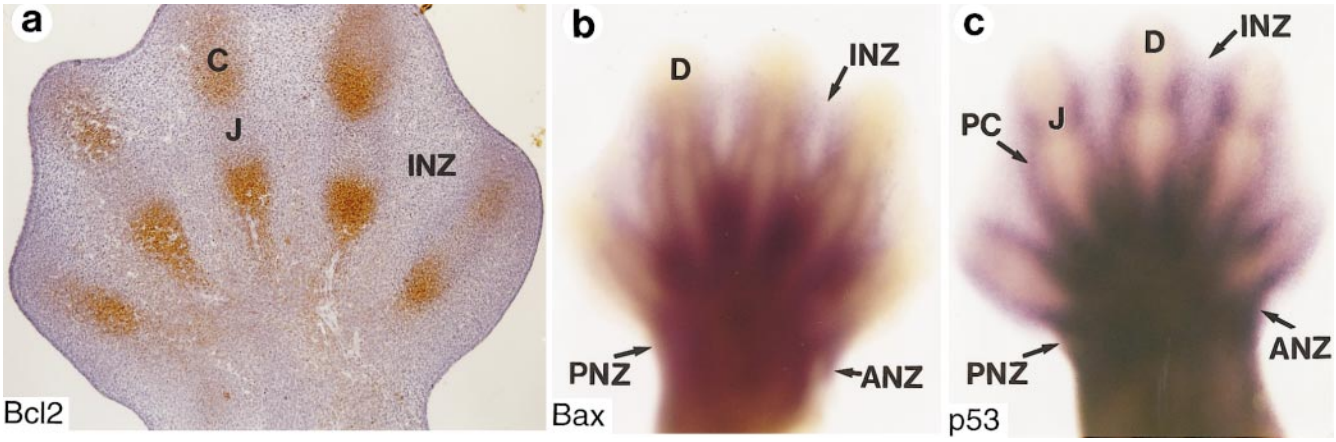

FIG. 3. Detection of the Bc12 protein and of *Bax* and *p53* transcripts in E13.5 WT hindlimbs. Note the complementary distributions of Bc12 in the precartilaginous condensation and of *Bax* and *p53* in the necrotic zones. ANZ, anterior necrotic zone; C, cartilage condensation; D, digit; INZ, interdigital necrotic zone; J, forming joint; PC, perichondrium; PNZ, posterior necrotic zone. Magnifications, ×85 (a); ×65 (b and c).

Stromelysin-3 is a secreted enzyme. It belongs to the matrix metalloproteinase family which has been implicated in a variety of tissue remodeling processes (reviewed in Basset *et al.*, 1997). In the present study we found that expression of stromelysin-3 first appears in the (prospective) necrotic zones at E12.5 (data not shown), where it is increased at E13.5 (Lefebvre *et al.*, 1995; Fig. 4h). At E13.5 stromelysin-3 expression was specifically decreased in the INZ of $A\beta^{+/-}/A\gamma$ autopods (Fig. 4i), while it was almost abrogated in the INZs of $A\beta/A\gamma$ autopods (Fig. 4j).

RARβ and RARγ Are Implicated in the Anteroposterior Patterning of the Limb

Approximately 10% (3 of 35) of the E13.5 $A\beta/A\gamma$ mutants displayed an additional, unilateral or bilateral, preaxial digit on the hindlimb (Fig. 6a). This abnormality was never observed in the 357 littermates of these double null fetuses (which included 40 $A\beta^{+/-}/A\gamma$ fetuses). Interestingly, BMP-7-deficient mice display the same preaxial polydactyly of the hindlimb (Luo *et al.*, 1995; Dudley *et al.*, 1995), which suggests the involvement of BMP-7 in early limb bud shaping (Luo *et al.*, 1995; Hofmann *et al.*, 1996). Therefore, we further investigated the distribution of *BMP-7* transcripts at earlier developmental stages. During normal development, the *BMP-7* pattern of expression in the limb bud is very dynamic. At E11.5 it is restricted to the mesenchyme and is strong in the posterior region (Fig. 6b; see also Hofmann *et al.*, 1996). The expression of *BMP-7* was markedly decreased in forelimb and hindlimb autopods of E11.5 $A\beta/A\gamma$ mutants (Fig. 6c; and data not shown). In contrast, no decrease was observed in other sites where *BMP-7* is normally expressed, including the otic vesicle, pharyngeal clefts, heart, and precartilaginous condensations (data not shown; see Lyons *et al.*, 1995).

DISCUSSION

Involvement of Tissue Transglutaminase and of Stromelysin-3 in Retinoic Acid-Dependent Physiological Cell Death

Several lines of evidences have suggested that RA could be instrumental in controlling PCD in developing limb buds: (i) limb reduction defects and cartilaginous syndactyly observed following systemic administration of pharmacological doses of either vitamin A or RA are caused, at least in part, by an expansion of regions of PCD (Kochhar, 1973; Alles and Sulik, 1989); (ii) cell death induced by excess RA in the INZs, ANZ, and PNZ is characterized by apoptotic features similar to those occurring naturally in PCD in the normal developing limb, i.e., the presence of apoptotic bodies, DNA fragmentation, and activation of phagocytic cells (Ahuja *et al.*, 1997); (iii) administration of RA can rescue the soft tissue syndactyly which represents the hallmark of the *Hammertoe* mutant mouse phenotype, through restoring apoptosis (Ahuja *et al.*, 1997); (iv) fetal mouse limbs cultured in a chemically defined, retinoid-deficient medium display interdigital webbing which can be prevented by physiological concentrations of RA (Lussier *et al.*, 1993).

In the present study, we show that the complete lack of digit separation in $A\beta/A\gamma$ mutants can be ascribed to reduction of apoptosis and to maintenance of a proliferative state in the INZs. These results indicate that RARβ and RARγ mediate the apoptotic effects of RA in the INZs, possibly via a cross-talk between the interdigital mesenchyme (the site of RARβ expression) and either the autopod ectoderm (see Hurle and Ganan, 1986) or the precartilaginous condensation of the digits (the two main sites of RARγ expression, see Introduction). They also suggest that RA

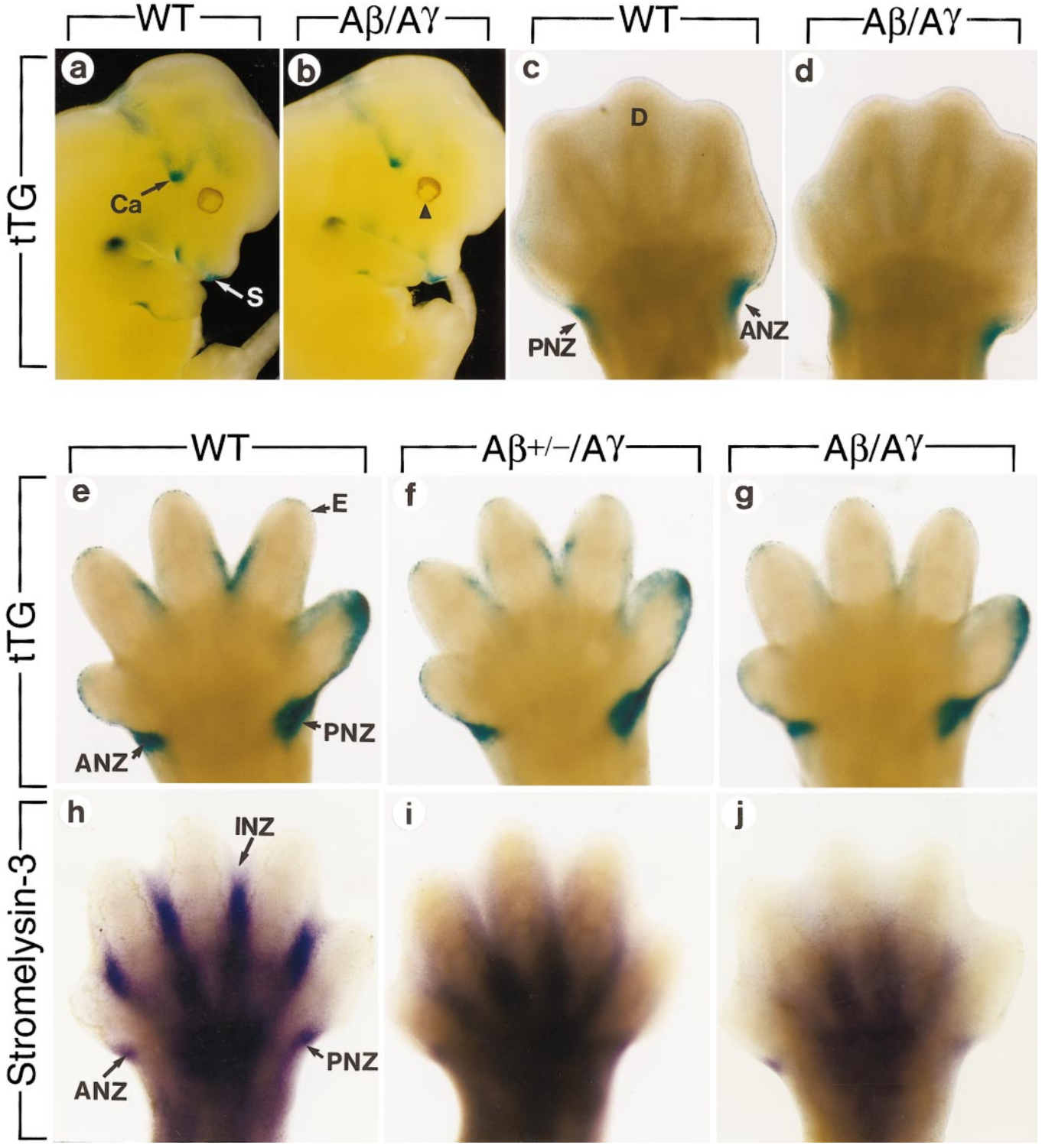

FIG. 4. Comparison of tissue transglutaminase (tTG) promoter activity and stromelysin-3 transcripts distribution in WT, $A\beta^{+/-}/A\gamma$, and $A\beta/A\gamma$ mutants at E12.5 (a–d), E14.0 (e–g), and E13.5 (h–j). (a and b) Lateral views of the cephalic region. (c–g) Ventral view of forelimbs. (h–j) Dorsal view of forelimbs. Note the specific down-regulation of tTG promoter activity in the INZs, whose timing is coincident with the process of digit separation. Note also the graded decrease of the tTG promoter activity and stromelysin-3 transcript level upon removal of one or both alleles of RARβ in the RARγ null genetic background. ANZ, anterior necrotic zone; Ca, calvaria; D, digit; E, ectoderm; INZ, interdigital necrotic zone; PNZ, posterior necrotic zone; S, snout. The arrowhead in (b) points to the abnormal $A\beta/A\gamma$ mutant eye. Magnifications, ×15 (a and b); ×110 (c and d); ×60 (e–g); ×65 (h–j).

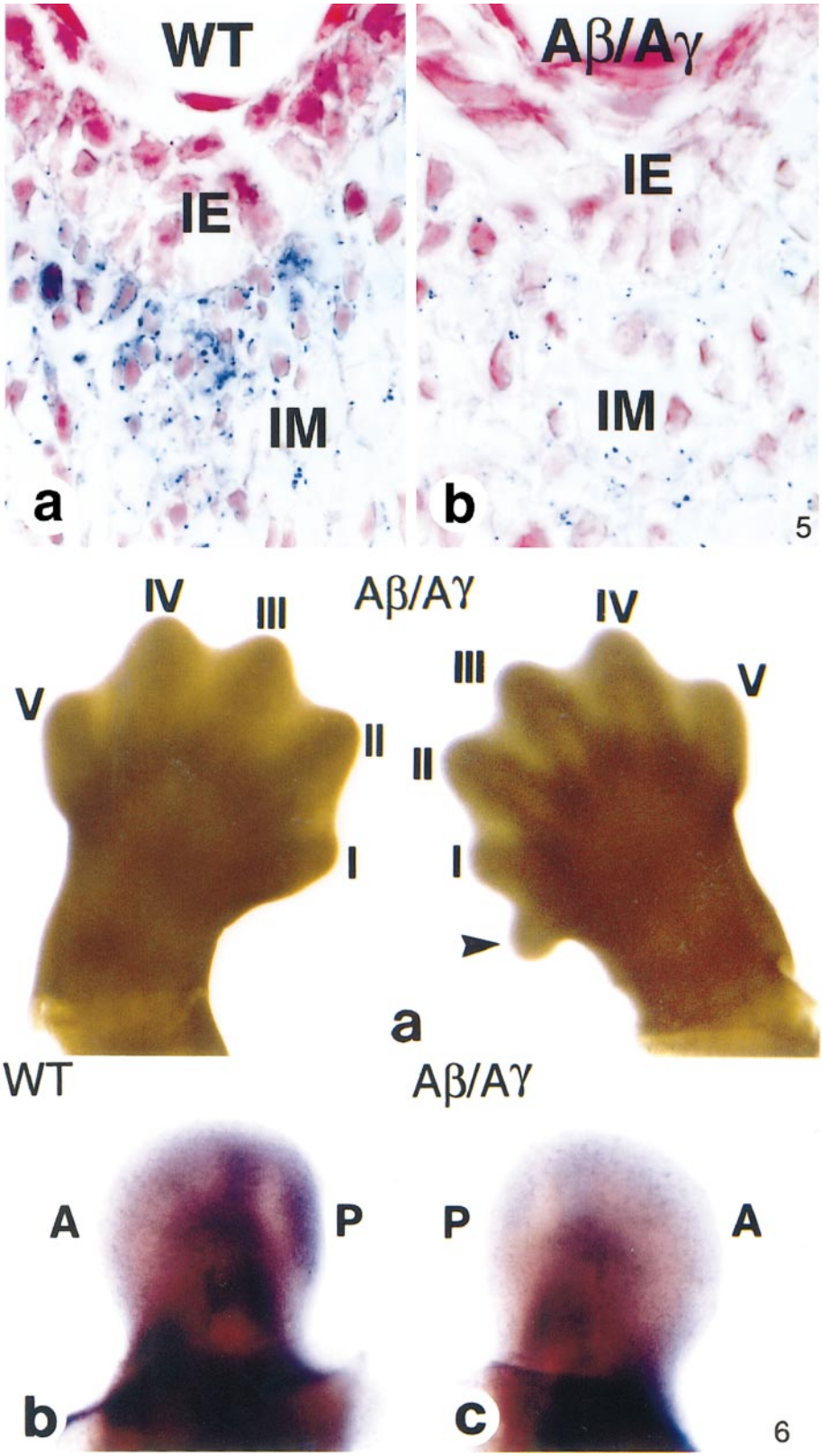

FIG. 5. Comparison of tissue transglutaminase (tTG) promoter activity on histological sections through the third interdigital space of WT and Aβ/Aγ forelimbs displayed in Fig. 4e. The relative abundance of the β-galactosidase reaction product (blue) associated with a nucleus (red) is proportional to the activity of the tTG promoter within cells. IE, interdigital epithelium; IM, interdigital mesenchyme. Magnifications, ×400.

may act as an antiproliferative factor in interdigital mesenchymal cells. Unexpectedly, the reduced PCD was not paralleled by a decrease in the number of macrophages which, under normal conditions, phagocytose the debris of dead mesenchymal cells (Hopkinson-Woodley *et al.,* 1994 and references therein). This finding indicates that the chemotactic cues, which presumably recruit monocyte-derived macrophages at the sites of PCD, may still be produced in Aβ/Aγ autopods, despite the rarity of dying cells.

The patterns of *BMP-2* and *BMP-4* expression were qualitatively and quantitatively unaffected in the necrotic zones of Aβ/Aγ mice, suggesting that RA acts either downstream or independently of these BMPs in controlling PCD in the autopod. In contrast, *BMP-7* expression was markedly reduced in the autopods of Aβ/Aγ mutants at E11.5, E12.5, and E13.5. However, down-regulation of *BMP-7* expression was not directly correlated to reduction of interdigital apoptosis since (i) it was clearly not restricted to the interdigital mesenchyme and (ii) it was not found in $A\beta^{+/-}$/Aγ mutants (which display a 100% penetrance of webbing between all digits). Similar to those of *BMP-2* and *BMP-4*, the expression patterns of *Msx-1* and *Msx-2* and of four *AbdB*-related *Hox* genes were unaffected in Aβ/Aγ autopods.

The present results confirm the findings that *Bcl2* is normally expressed in the digital rays only (Novack and Korsmeyer, 1994) and show that *Bax* transcripts are expressed in the necrotic zones only. Thus, in the mesoderm-derived structures of the autopod, expression patterns of *Bcl2* and *RARγ* on the one hand and of *Bax* and *RARβ* on the other hand are complementary and correlated with the distribution of surviving and dying cells, respectively. Our data showing that *p53* and *Bax* transcripts are colocalized in the necrotic zones support the possibility that p53 could control *Bax* expression in these zones (Miyashita *et al.,* 1994; Miyashita and Reed, 1995). However, the levels and domains of expression of *Bcl2*, *Bax*, and *p53* were unaffected in Aβ/Aγ autopods, indicating that other members of the Bcl2/Bax family (Boise *et al.,* 1993) are most probably involved in RA-dependent interdigital apoptosis. In this respect it is interesting to note that the complete lack of Bcl2 is, by itself, not sufficient to induce limb malformations (Veis *et al.,* 1993).

Cells committed to death initiate a cascade of biochemical events leading to their destruction. This cascade involves notably the cytosolic enzyme, tissue transglutaminase (tTG). Expression of tTG is a precocious feature of cells which are committed to apoptosis (Fesus *et al.,* 1987; Piacentini *et al.,* 1991), in which it catalyzes the irreversible cross-linking of intracellular proteins. Through this action, it might prevent cellular disintegration prior to phagocytosis (Fesus *et al.,* 1987), but also represent a killer effector element of the apoptotic program. Inhibition of tTG expression by antisense cDNA in cell cultures is sufficient to decrease both spontaneous and RA-induced apoptosis (Melino *et al.,* 1994), whereas an increase of tTG expression in cell lines to levels comparable to those measured in apoptotic cells *in vivo* induces cytoplasmic condensation followed by the blebbing and fragmentation characteristic of apoptosis (Gentile *et al.,* 1992; Melino *et al.,* 1994). RA in excess increases tTG activity in many cultured cells (Zhang *et al.,* 1995), and the initiation of RA-induced cell death in the mesenchyme of the chick limb bud is accompanied by a transient increase in tTG activity (Jiang and Kochhar, 1992). Retinoids increase transcription of the mouse tTG gene through a *cis*-acting response element located in the promoter region (Nagy *et al.,* 1996a, 1997). The decrease of tTG promoter activity in INZ cells of RARβ/RARγ compound mutants strongly suggests that expression of the corresponding gene in these cells is normally regulated by RA *in vivo*. These data also raise the possibility that an autocrine or paracrine retinoid signal might trigger apoptosis upon direct activation of the tTG promoter. In this respect it is interesting to note that retinaldehyde dehydrogenase type 2 (RALDH-2), a major retinoic acid generating enzyme, is strongly and specifically expressed in the interdigital mesenchyme before and during the formation of the INZs (Niederreither *et al.,* 1997).

Stromelysin-3 is a matrix metalloproteinase whose expression has been associated with tissue remodeling processes characterized by extensive extracellular matrix turnover during embryonic development, wound healing, or tumor invasion (Lefebvre *et al.,* 1992, 1995; Wang and Brown, 1993; Patterson *et al.,* 1995). It is strongly expressed during postweaning involution of the mouse mammary gland (Lefebvre *et al.,* 1992), a process known to involve intense apoptosis (Streuli *et al.,* 1991). It is also expressed in the interdigital spaces (Lefebvre *et al.,* 1995; Masson *et al.,* 1998), concomitantly with the appearance of the first apoptotic cells (present report). Down-regulation of stromelysin-3 in the INZs of $A\beta^{+/-}$/Aγ and Aβ/Aγ mutants cannot account on its own for the decrease in apoptosis, since stromelysin-3 null mice have normal limbs (Masson *et al.,* 1998). However, modulation of stromelysin-3 expression by RA *in vivo* could provide a mechanism for the coupling of cell death and extracellular matrix remodeling in the INZs.

FIG. 6. Preaxial polydactyly and decreased *BMP-7* expression in Aβ/Aγ autopods. (a) Dorsal view of the hindlimbs of a E13.5 Aβ/Aγ mutant, illustrating a case of unilateral preaxial polydactyly. Note that the supernumerary preaxial digit (arrowhead) always displayed a cartilaginous nodule on histological sections. (b and c) Dorsal views of E11.5 hindlimbs showing a decrease of *BMP-7* expression levels prior to the formation of the digits. A, anterior; P, posterior; (I–V) digit 1 (the most anterior) to digit 5 (the most posterior). The arrowhead in (a) points to the supernumerary preaxial digit. Magnifications, ×36 (a), ×135 (b and c).

That cell death, tTG, and stromelysin-3 expression are decreased in all INZs, but not in the ANZ and PNZ of $A\beta^{+/-}/A\gamma$ and $A\beta/A\gamma$ mutants, suggests a fundamental difference between these three necrotic zones.

BMP-7 May Act Downstream of RA in the Patterning of the Limb

The teratogenic effects of RA administration first suggested that RA is involved in limb morphogenesis. Topical administration of RA can mimic the effects of the zone of polarizing activity in the chick (reviewed by Tickle and Eichele, 1994) and induces postaxial polydactyly in the regenerating forelimbs of newt (Thoms and Stocum, 1984). Systemic administration of RA in excess enhances the incidence of postaxial polydactyly in the mouse (Bynum, 1991, and references therein). The penetrance of RA-induced limb defects is decreased in mouse embryos lacking RXRα (Sucov *et al.*, 1995). The physiological effects of RA on limb patterning have been deduced from knock-outs of retinoid receptors and binding proteins (CRABPs). $A\alpha/A\gamma$ mutants display forelimb malformations, the majority of which involve a loss of anterior skeletal elements (Lohnes *et al.*, 1994). Similar defects have been found in compound mutants in which an RXRα mutation abrogating the AF-2 activation function is associated with a RARγ null mutation (Mascrez *et al.*, 1998). About half of the CRABPII null mutants exhibit a postaxial digit rudiment located, in general, on the forelimb; the penetrance of this abnormality is increased to 80% in CRABPI/CRABPII double null mutants, 13% of which show, in addition, an extra preaxial digit rudiment (Lampron *et al.*, 1995). In the present study, we report the occurrence in ~10% of the $A\beta/A\gamma$ mice of a supernumerary preaxial digit on the hindlimb only. The same phenotype is observed in 25 to 80% of the BMP-7 null mutant mice, depending on the genetic background (Dudley *et al.*, 1995; Luo *et al.*, 1995). *BMP-7* expression is specifically down-regulated in the limbs of $A\beta/A\gamma$ mutants at E11.5, E12.5, and E13.5. In contrast, a down-regulation of *BMP-7* expression is not observed in $A\beta^{+/-}/A\gamma$ mutants which never displayed limb patterning defects. Altogether, these data strongly suggest that the decreased expression of *BMP-7* is causally related to the formation of the supernumerary digit in $A\beta/A\gamma$ mutants and, therefore, that RA may exert some of its effects on anteroposterior patterning of the limb through controlling *BMP-7* expression. That mutations in specific pairs of RARs or in CRABPs can preferentially or exclusively disturb pattern formation in the forelimb or in the hindlimb is in keeping with the notion that "armness" and "legness" are encoded by distinct subsets of genes (review Schwabe *et al.*, 1998).

ACKNOWLEDGMENTS

We are grateful to Drs. R. Beddington, P. Dollé, D. Duboule, R. Hill, B. Hogan, J. Jenkins, S. Korsmeyer, and M.C. Rio for providing us with cDNA probes and to Dr. Gordon for F4/80 monoclonal antibody. We thank B. Weber, C. Fisher, I. Tilly, and B. Bondeau for technical assistance and Jean-Luc Vonesch and secretarial staff for their help in the preparation of the manuscript. This work was supported by funds from the Centre National de la Recherche Scientifique (CNRS), the Institut National de la Santé et de la Recherche Médicale (INSERM), the Hôpital Universitaire de Strasbourg, the Collège de France, the Association pour la Recherche sur le Cancer (ARC), the Fondation pour la Recherche Medicale (FRM), the Ligue Nationale contre le Cancer, the Human Frontier Science Program, Bristol Myers Squibb, EEC Contract FAIR-CT97-3220, and NIH Grant CA76088. V.D. was supported by an ARC fellowship.

REFERENCES

Agarwal, N., and Mehta, K. (1997). Possible involvement of Bcl-2 pathway in retinoid X receptor α-induced apoptosis of HL-60 cells. *Biochem. Biophys. Res. Commun.* **230,** 251–253.

Ahuja, H. S., James, W., and Zakeri, Z. (1997). Rescue of the limb deformity in *hammertoe* mutant mice by retinoic acid-induced cell death. *Dev. Dyn.* **208,** 466–481.

Alles, A. J., and Sulik, K. K. (1989). Retinoic-acid-induced limb-reduction defects: Perturbation of zones of programmed cell death as a pathogenetic mechanism. *Teratology* **40,** 163–171.

Arkell, R., and Beddington, R. S. (1997). BMP-7 influences pattern and growth of the developing hindbrain of mouse embryos. *Development* **124,** 1–12.

Austyn, J. M., and Gordon, S. (1981). F4/80, a monoclonal antibody directed specifically against the mouse macrophage. *Eur. J. Immunol.* **11,** 805–815.

Basset, P., Bellocq, J. P., Lefebvre, O., Noel, A., Chenard, M. P., Wolf, C., Anglard, P., and Rio, M. C. (1997). Stromelysin-3: A paradigm for stroma-derived factors implicated in carcinoma progression. *Crit. Rev. Onco/Hematol.* **26,** 43–53.

Boise, L. H., Gonzalez-Garcia, M., Postema, C. E., Ding, L., Lindsten, T., Turka, L. A., Mao, X., Nunez, G., and Thompson, C. B. (1993). bcl-x, a bcl-2-related gene that functions as a dominant regulator of apoptotic cell death. *Cell* **74,** 597–608.

Bynum, S. V. (1991). Morphogenesis of retinoic acid-induced postaxial polydactyly in mice. *Teratology* **43,** 1–9.

Chambon, P. (1996). A decade of molecular biology of retinoic acid receptors. *FASEB. J.* **10,** 940–954.

Coelho, C. N., Sumoy, L., Kosher, R. A., and Upholt, W. B. (1992). *GHox-7*: A chicken homeobox-containing gene expressed in a fashion consistent with a role in patterning events during embryonic chick limb development. *Differentiation* **49,** 85–92.

Coelho, C. N., Sumoy, L., Rodgers, B. J., Davidson, D. R., Hill, R. E., Upholt, W. B., and Kosher, R. A. (1991). Expression of the chicken homeobox-containing gene *GHox-8* during embryonic chick limb development. *Mech. Dev.* **34,** 143–154.

Conlon, R. A., and Rossant, J. (1992). Exogenous retinoic acid rapidly induces anterior ectopic expression of murine *Hox-2* genes *in vivo*. *Development* **116,** 357–368.

Davis, A. P., and Capecchi, M. R. (1994). Axial homeosis and appendicular skeleton defects in mice with a targeted disruption of *hoxd-11*. *Development* **120,** 2187–2198.

Debbas, M., and White, E. (1993). Wild-type p53 mediates apoptosis by E1A, which is inhibited by E1B. *Genes Dev.* **7,** 546–554.

Dollé, P., Dierich, A., Le Meur, M., Schimmang, T., Schuhbaur, B., Chambon, P., and Duboule, D. (1993). Disruption of the *Hoxd-13*

gene induces localized heterochrony leading to mice with neotenic limbs. *Cell* **75,** 431–441.

Dollé, P., Fraulob, V., Kastner, P., and Chambon, P. (1994). Developmental expression of murine retinoid X receptor (RXR) genes. *Mech. Dev.* **45,** 91–104.

Dollé, P., Izpisua-Belmonte, J. C., Boncinelli, E., and Duboule, D. (1991). The *Hox-4.8* gene is localized at the 5′ extremity of the *Hox-4* complex and is expressed in the most posterior parts of the body during development. *Mech. Dev.* **36,** 3–13.

Dollé, P., Izpisua-Belmonte, J. C., Falkenstein, H., Renucci, A., and Duboule, D. (1989a). Coordinate expression of the murine Hox-5 complex homoeobox-containing genes during limb pattern formation. *Nature* **342,** 767–772.

Dollé, P., Ruberte, E., Kastner, P., Petkovich, M., Stoner, C. M., Gudas, L. J., and Chambon, P. (1989b). Differential expression of genes encoding α, β and γ retinoic acid receptors and CRABP in the developing limbs of the mouse. *Nature* **342,** 702–705.

Dudley, A. T., Lyons, K. M., and Robertson, E. J. (1995). A requirement for bone morphogenetic protein-7 during development of the mammalian kidney and eye. *Genes Dev.* **9,** 2795–2807.

Favier, B., Rijli, F. M., Fromental-Ramain, C., Fraulob, V., Chambon, P., and Dollé, P. (1996). Functional cooperation between the non-paralogous genes *Hoxa-10* and *Hoxd-11* in the developing forelimb and axial skeleton. *Development* **122,** 449–460.

Fesus, L., Tarcsa, E., Kedei, N., Autuori, F., and Piacentini, M. (1991). Degradation of cells dying by apoptosis leads to accumulation of epsilon(gamma-glutamyl)lysine isodipeptide in culture fluid and blood. *FEBS Lett.* **284,** 109–112.

Fesus, L., Thomazy, V., and Falus, A. (1987). Induction and activation of tissue transglutaminase during programmed cell death. *FEBS Lett.* **224,** 104–108.

Francis, P. H., Richardson, M. K., Brickell, P. M., and Tickle, C. (1994). Bone morphogenetic proteins and a signaling pathway that controls patterning in the developing chick limb. *Development* **120,** 209–218.

Fromental-Ramain, C., Warot, X., Messadecq, N., Le Meur, M., Dollé, P., and Chambon, P. (1996). *Hoxa-13* and *Hoxd-13* play a crucial role in the patterning of the limb autopod. *Development* **122,** 2997–3011.

Ganan, Y., Macias, D., Duterque-Coquillaud, M., Ros, M. A., and Hurle, J. M. (1996). Role of TGF β s and BMPs as signals controlling the position of the digits and the areas of interdigital cell death in the developing chick limb autopod. *Development* **122,** 2349–2357.

Gavrieli, Y., Sherman, Y., and Ben-Sasson, S. A. (1992). Identification of programmed cell death in situ via specific labeling of nuclear DNA fragmentation. *J. Cell Biol.* **119,** 493–501.

Gentile, V., Thomazy, V., Piacentini, M., Fesus, L., and Davies, P. J. A. (1992). Expression of tissue transglutaminase in balb-C 3T3 fibroblasts: Effects on cellular morphology and adhesion. *J. Cell Biol.* **119,** 463–474.

Ghyselinck, N. B., Dupé, V., Dierich, A., Messaddeq, N., Garnier, J. M., Rochette-Egly, C., Chambon, P., and Mark, M. (1997). Role of the retinoic acid receptor beta (RARβ) during mouse development. *Int. J. Dev. Biol.* **41,** 425–447.

Graham, A., Francis-West, P., Brickell, P., and Lumsden, A. (1994). The signalling molecule BMP4 mediates apoptosis in the rhombencephalic neural crest. *Nature* **372,** 684–686.

Helder, M. N., Ozkaynak, E., Sampath, K. T., Luyten, F. P., Latin, V., Oppermann, H., and Vukicevic, S. (1995). Expression pattern of osteogenic protein-1 (bone morphogenetic protein-7) in human and mouse development. *J. Histochem. Cytochem.* **43,** 1035–1044.

Hill, R. E., Jones, P. F., Rees, A. R., Sime, C. M., Justice, M. J., Copeland, N. G., Jenkins, N. A., Graham, E., and Davidson, D. R. (1989). A new family of mouse homeo box-containing genes: Molecular structure, chromosomal location, and developmental expression of Hox-7.1. *Genes Dev.* **3,** 26–37.

Hinchliffe, J. R. (1981). Cell death in embryogenesis. *In* "Cell Death in Biology and Pathology" (I. D. Bowen and R. A. Lockshin, Eds.), pp. 35–69. Chapman and Hall, London.

Hofmann, C., Luo, G., Balling, R., and Karsenty, G. (1996). Analysis of limb patterning in BMP-7 deficient mice. *Dev. Genet.* **19,** 43–50.

Hogan, B. L. (1996). Bone morphogenetic proteins in development. *Curr. Opin. Genet. Dev.* **6,** 432–438.

Hopkinson-Woolley, J., Hughes, D., Gordon, S., and Martin, P. (1994). Macrophage recruitment during limb development and wound healing in the embryonic and foetal mouse. *J. Cell Sci.* **107,** 1159–1167.

Hurle, J. M., and Ganan, Y. (1986). Interdigital tissue chondrogenesis induced by surgical removal of the ectoderm in the embryonic chick leg bud. *J. Embryol. Exp. Morphol.* **94,** 231–244.

Jenkins, J. R., Rudge, K., Redmond, S., and Wade-Evans, A. (1984). Cloning and expression analysis of full length mouse cDNA sequences encoding the transformation associated protein p53. *Nucleic Acids Res.* **12,** 5609–5626.

Jiang, H., and Kochhar, D. M. (1992). Induction of tissue transglutaminase and apoptosis by retinoic acid in the limb bud. *Teratology* **46,** 333–340.

Jones, C. M., Lyons, K. M., and Hogan, B. L. (1991). Involvement of bone morphogenetic protein-4 (BMP-4) and Vgr-1 in morphogenesis and neurogenesis in the mouse. *Development* **111,** 531–542.

Kastner, P., Grondona, J. M., Mark, M., Gansmuller, A., Le Meur, M., Decimo, D., Vonesch, J. L., Dollé, P., and Chambon, P. (1994). Genetic analysis of RXR α developmental function: Convergence of RXR and RAR signaling pathways in heart and eye morphogenesis. *Cell* **78,** 987–1003.

Kastner, P., Mark, M., Ghyselinck, N., Krezel, W., Dupé, V., Grondona, J. M., and Chambon, P. (1997). Genetic evidence that the retinoid signal is transduced by heterodimeric RXR/RAR functional units during mouse development. *Development* **124,** 313–326.

Kochhar, D. M. (1973). Limb development in mouse embryos. I. Analysis of teratogenic effects of retinoic acid. *Teratology* **7,** 289–298.

Krajewski, S., Krajewska, M., Shabaik, A., Miyashita, T., Wang, H. G., and Reed, J. C. (1994). Immunohistochemical determination of *in vivo* distribution of Bax, a dominant inhibitor of Bcl-2. *Am. J. Pathol.* **145,** 1323–1336.

Lampron, C., Rochette-Egly, C., Gorry, P., Dollé, P., Mark, M., Lufkin, T., Le Meur, M., and Chambon, P. (1995). Mice deficient in cellular retinoic acid binding protein II (CRABPII) or in both CRABPI and CRABPII are essentially normal. *Development* **121,** 539–548.

Lefebvre, O., Regnier, C., Chenard, M. P., Wendling, C., Chambon, P., Basset, P., and Rio, M. C. (1995). Developmental expression of mouse stromelysin-3 mRNA. *Development* **121,** 947–955.

Lefebvre, O., Wolf, C., Limacher, J. M., Hutin, P., Wendling, C., Le Meur, M., Basset, P., and Rio, M. C. (1992). The breast cancer-associated stromelysin-3 gene is expressed during mouse mammary gland apoptosis. *J. Cell Biol.* **119,** 997–1002.

Lohnes, D., Kastner, P., Dierich, A., Mark, M., Le Meur, M., and Chambon, P. (1993). Function of retinoic acid receptor γ in the mouse. *Cell* **73,** 643–658.

Lohnes, D., Mark, M., Mendelsohn, C., Dollé, P., Dierich, A., Gorry, P., Gansmuller, A., and Chambon, P. (1994). Function of the retinoic acid receptors (RARs) during development (I). Craniofacial and skeletal abnormalities in RAR double mutants. *Development* **120,** 2723–2748.

Lufkin, T., Lohnes, D., Mark, M., Dierich, A., Gorry, P., Gaub, M. P., Le Meur, M., and Chambon, P. (1993). High postnatal lethality and testis degeneration in retinoic acid receptor α mutant mice. *Proc. Natl. Acad. Sci. USA* **90,** 7225–7229.

Luo, G., Hofmann, C., Bronckers, A. L., Sohocki, M., Bradley, A., and Karsenty, G. (1995). BMP-7 is an inducer of nephrogenesis, and is also required for eye development and skeletal patterning. *Genes Dev.* **9,** 2808–2820.

Lussier, M., Canoun, C., Ma, C., Sank, A., and Shuler, C. (1993). Interdigital soft tissue separation induced by retinoic acid in mouse limbs cultured in vitro. *Int. J. Dev. Biol.* **37,** 555–564.

Lyons, K. M., Hogan, B. L., and Robertson, E. J. (1995). Colocalization of BMP 7 and BMP 2 RNAs suggests that these factors cooperatively mediate tissue interactions during murine development. *Mech. Dev.* **50,** 71–83.

Lyons, K. M., Pelton, R. W., and Hogan, B. L. (1990). Organogenesis and pattern formation in the mouse: RNA distribution patterns suggest a role for bone morphogenetic protein-2A (BMP-2A). *Development* **109,** 833–844.

Macias, D., Ganan, Y., Sampath, T. K., Piedra, M. E., Ros, M. A., and Hurle, J. M. (1997). Role of BMP-2 and OP-1 (BMP-7) in programmed cell death and skeletogenesis during chick limb development. *Development* **124,** 1109–1117.

Maconnachie, E. (1979). A study of digit fusion in the mouse embryo. *J. Embryol. Exp. Morphol.* **49,** 259–276.

Mascrez, B., Mark, M., Dierich, A., Ghyselinck, N., Kastner, P., and Chambon, P. (1998). The RXRα ligand-dependent activation function (AF-2) is important for mouse development. *Development* **125,** 4691–4707.

Masson, R., Lefebvre, O., Noël A., El Fahime, M., Chenard, M. P., Wendling, C., Kebers, F., LeMeur, M., Dierich, A., Foidart, J. M., Basset, P., and Rio, M. C. (1998). *In vivo* evidence that the stromelysin-3 metalloproteinase contributes in a paracrine manner to epithelial cell malignancy. *J. Cell. Biol,* in press.

Melino, G., Annicchiarico-Petruzzelli, M., Piredda, L., Candi, E., Gentile, V., Davies, P. J., and Piacentini, M. (1994). Tissue transglutaminase and apoptosis: Sense and antisense transfection studies with human neuroblastoma cells. *Mol. Cell. Biol.* **14,** 6584–6596.

Mendelsohn, C., Lohnes, D., Decimo, D., Lufkin, T., Le Meur, M., Chambon, P., and Mark, M. (1994). Function of the retinoic acid receptors (RARs) during development (II). Multiple abnormalities at various stages of organogenesis in RAR double mutants. *Development* **120,** 2749–2771.

Mendelsohn, C., Ruberte, E., Le Meur, M., Morriss-Kay, G., and Chambon, P. (1991). Developmental analysis of the retinoic acid-inducible RAR-β2 promoter in transgenic animals. *Development* **113,** 723–734.

Merino, R., Ding, L., Veis, D. J., Korsmeyer, S. J., and Nunez, G. (1994). Developmental regulation of the Bcl-2 protein and susceptibility to cell death in B lymphocytes. *EMBO J.* **13,** 683–691.

Miyashita, T., and Reed, J. C. (1995). Tumor suppressor p53 is a direct transcriptional activator of the human *bax* gene. *Cell* **80,** 293–299.

Miyashita, T., Krajewski, S., Krajewska, M., Wang, H. G., Lin, H. K., Liebermann, D. A., Hoffman, B., and Reed, J. C. (1994). Tumor suppressor p53 is a regulator of *bcl-2* and *bax* gene expression in vitro and in vivo. *Oncogene* **9,** 1799–1805.

Monczak, Y., Trudel, M., Lamph, W. W., and Miller, W. H., Jr. (1997). Induction of apoptosis without differentiation by retinoic acid in PLB-985 cells requires the activation of both RAR and RXR. *Blood* **90,** 3345–3355.

Morgenbesser, S. D., Williams, B. O., Jacks, T., and De Pinho, R. A. (1994). p53-dependent apoptosis produced by Rb-deficiency in the developing mouse lens. *Nature* **371,** 72–74.

Nagy, L., Saydak, M., Shipley, N., Lu, S., Basilion, J. P., Yan, Z. H., Syka, P., Chandraratna, R. A. S., Heyman, R. A., Stein, J. P., and Davies, P. J. A. (1996a). Identification and characterization of a versatile retinoid response element (RARE/RXRE) in the mouse tissue transglutaminase gene promoter. *J. Biol. Chem.* **271,** 4355–4365.

Nagy, L., Thomazy, V. A., Chandraratna, R. A., Heyman, R. A., and Davies, P. J. (1996b). Retinoid-regulated expression of *BCL-2* and tissue transglutaminase during the differentiation and apoptosis of human myeloid leukemia (HL-60) cells. *Leukemia Res.* **20,** 499–505.

Nagy, L., Thomazy, V. A., Saydak, M. M., Stein, J. P., and Davies, P. J. A. (1997). The promoter of the mouse tissue transglutaminase gene directs tissue-specific, retinoid-regulated and apoptosis-linked expression. *Cell Death Differ.* **4,** 534–547.

Niederreither, K., McCaffery, P., Dräger, U. C., Chambon, P., and Dollé, P. (1997). Restricted expression and retinoic acid-induced downregulation of the retinaldehyde dehydrogenase type 2 (RALDH-2) gene during mouse development. *Mech. Dev.* **62,** 67–78.

Novack, D. V., and Korsmeyer, S. J. (1994). Bcl-2 protein expression during murine development. *Am. J. Pathol.* **145,** 61–73.

Nunez, G., London, L., Hockenbery, D., Alexander, M., McKearn, J. P., and Korsmeyer, S. J. (1990). Deregulated *Bcl-2* gene expression selectively prolongs survival of growth factor-deprived hemopoietic cell lines. *J. Immunol.* **144,** 3602–3610.

Oltvai, Z. N., Milliman, C. L., and Korsmeyer, S. J. (1993). Bcl-2 heterodimerizes in vivo with a conserved homolog, Bax, that accelerates programmed cell death. *Cell* **74,** 609–619.

Patterton, D., Hayes, W. P., and Shi, Y. B. (1995). Transcriptional activation of the matrix metalloproteinase gene stromelysin-3 coincides with thyroid hormone-induced cell death during frog metamorphosis. *Dev. Biol.* **167,** 252–262.

Piacentini, M., Autuori, F., Dini, L., Farrace, M. G., Ghibelli, L., Piredda, L., and Fesus, L. (1991). "Tissue" transglutaminase is specifically expressed in neonatal rat liver cells undergoing apoptosis upon epidermal growth factor-stimulation. *Cell Tissue Res.* **263,** 227–235.

Robert, B., Lyons, G., Simandl, B. K., Kuroiwa, A., and Buckingham, M. (1991). The apical ectodermal ridge regulates *Hox-7* and *Hox-8* gene expression in developing chick limb buds. *Genes Dev.* **5,** 2363–2374.

Ros, M. A., Lyons, G. E., Mackem, S., and Fallon, J. F. (1994). Recombinant limbs as a model to study homeobox gene regulation during limb development. *Dev. Biol.* **166,** 59–72.

Schwabe, J. W. R., Rodriguez-Esteban, C., and Izpisua Belmonte, J. C. (1998). Limbs are moving: Where are they going? *Trends Genet.* **14,** 229–235.

Schweichel, J. U., and Merker, H. J. (1973). The morphology of various types of cell death in prenatal tissues. *Teratology* **7,** 253–266.

Streuli, C. H., Bailey, N., and Bissel, M. J. (1991). Control of mammary epithelial differentiation: Basement membrane induces tissue-specific gene expression in the absence of cell–cell interaction and morphological polarity. *J. Cell Biol.* **115,** 1383–1395.

Sucov, H. M., Izpisua-Belmonte, J. C., Ganan, Y., and Evans, R. M. (1995). Mouse embryos lacking RXRα are resistant to retinoic-acid-induced limb defects. *Development* **121,** 3997–4003.

Suzuki, H. R., Padanilam, B. J., Vitale, E., Ramirez, F., and Solursh, M. (1991). Repeating developmental expression of *G-Hox 7*, a novel homeobox-containing gene in the chicken. *Dev. Biol.* **148,** 375–388.

Tickle, C., and Eichele, G. (1994). Vertebrate limb development. *Annu. Rev. Cell Biol.* **10,** 121–152.

Thoms, S. D., and Stocum, D. L. (1984). Retinoic acid-induced pattern duplication in regenerating urodele limbs. *Dev. Biol.* **103,** 319–328.

Vaux, D. L., Cory, S., and Adams, J. M. (1988). *Bcl-2* gene promotes haemopoietic cell survival and cooperates with c-myc to immortalize pre-B cells. *Nature* **335,** 440–442.

Veis, D. J., Sorenson, C. M., Shutter, J. R., and Korsmeyer, S. J. (1993). Bcl-2-deficient mice demonstrate fulminant lymphoid apoptosis, polycystic kidneys, and hypopigmented hair. *Cell* **75,** 229–240.

Wanek, N., Muneoka, K., Holler-Dinsmore, G., Burton, R., and Bryant, S. V. (1989). A staging system for mouse limb development. *J. Exp. Zool.* **249,** 41–49.

Wang, Z., and Brown, D. D. (1993). Thyroid hormone-induced gene expression program for amphibian tail resorption. *J. Biol. Chem.* **268,** 16270–16278.

Warot, X., Fromental-Ramain, C., Fraulob, V., Chambon, P., and Dollé, P. (1997). Gene dosage-dependent effects of the *hoxa-13* and *Hoxd-13* mutations on morphogenesis of the terminal parts of the digestive and urogenital tracts. *Development* **124,** 4781–4791.

Wood, H. B., Ward, S. J., and Morriss-Kay, G. (1996). Effects of all-*trans*-retinoic acid on skeletal pattern, 5′HoxD gene expression, and RARβ2/β4 promoter activity in embryonic mouse limbs. *Dev. Genet.* **18,** 74–84.

Yokouchi, Y., Sakiyama, J., Kameda, T., Iba, H., Suzuki, A., Ueno, N., and Kuroiwa, A. (1996). BMP-2/-4 mediate programmed cell death in chicken limb buds. *Development* **122,** 3725–3734.

Zakany, J., and Duboule, D. (1996). Synpolydactyly in mice with a targeted deficiency in the HoxD complex. *Nature* **384,** 69–71.

Zakeri, Z. F., and Ahuja, H. S. (1994). Apoptotic cell death in the limb and its relationship to pattern formation. *Biochem. Cell Biol.* **72,** 603–613.

Zhang, L. X., Mills, K. J., Dawson, M. I., Collins, S. J., and Jetten, A. M. (1995). Evidence for the involvement of retinoic acid receptor RARα-dependent signaling pathway in the induction of tissue transglutaminase and apoptosis by retinoids. *J. Biol. Chem.* **270,** 6022–6029.

Zou, H., and Niswander, L. (1996). Requirement for BMP signaling in interdigital apoptosis and scale formation. *Science* **272,** 738–741.

Received for publication September 3, 1998
Revised November 8, 1998
Accepted December 11, 1998